High-Q ring resonators directly written in As_2S_3 chalcogenide glass films

Shahar Levy,[1] Matvei Klebanov,[2] and Avi Zadok[1,*]

[1]*Faculty of Engineering, Bar-Ilan University, Ramat-Gan 5290002, Israel*
[2]*Department of Physics, Ben-Gurion University of the Negev, Beer-Sheva 8410501, Israel*
**Corresponding author: Avinoam.Zadok@biu.ac.il*

Received January 20, 2015; revised February 16, 2015; accepted February 16, 2015;
posted February 18, 2015 (Doc. ID 232805); published April 6, 2015

Planar ring resonator waveguides are fabricated in thin films of As_2S_3 chalcogenide glass, deposited on silica-on-silicon substrates. Waveguide cores are directly written by scanning the focused illumination of a femtosecond Ti:sapphire laser at a central wavelength of 810 nm, through a two-photon photo-darkening process. A large photo-induced index change of 0.3–0.4 refractive index units is obtained. The radius of the ring resonator is 1.9 mm, corresponding to a transmission free spectral range of 9.1 GHz. A high loaded (intrinsic) Q value of 110,000 (180,000) is achieved. The thermal dependence of the resonator transfer function is characterized. The results provide the first report, to the best of our knowledge, of directly written high-Q ring resonators in chalcogenide glass films, and demonstrate the potential of this simple technique towards the fabrication of planar lightguide circuits in these materials. © 2015 Chinese Laser Press

OCIS codes: (130.2755) Glass waveguides; (160.5335) Photosensitive materials; (230.5750) Resonators.
http://dx.doi.org/10.1364/PRJ.3.000063

1. INTRODUCTION

Chalcogenides are a category of glass compounds that contain one of the chalcogen elements: S, Se, or Te. Chalcogenides are drawing increased attention in research and applications, due to their remarkable electrical and optical properties. Although amorphous, they can be semiconducting and display bandgap behavior [1,2]; they are characterized by a broad transparency window, from the visible to the middle infrared [3]; their refractive index can be as high as 3.5 refractive index units (RIU) [4]; and their nonlinear refractive index, Raman scattering, and Brillouin scattering coefficients are 100–1000 times larger than the corresponding values in silica [4–6]. Lastly, chalcogenide glasses are highly photosensitive [7,8]: direct laser-beam illumination of these glasses could cause permanent material changes, ranging from refractive index variations [9,10] through to reflow and mass transfer [11–14], depending on wavelength and intensity. Chalcogenides therefore constitute a favorable material platform for all-optical signal processing and sensing applications [15–18].

Fabrication technologies of planar lightguide circuits (PLCs) in chalcogenide glasses include lithography and dry etching [19], lift-off processes [20], thermal nano-imprinting [21,22], and direct laser-beam writing [23–28]. Direct laser-beam writing relies on the photo-darkening effect in chalcogenides to introduce a local increase in the refractive index of core regions. The process is simple, does not involve the exposure of the glass materials to chemicals, and does not introduce sidewall roughness. On the other hand, linear losses of directly written waveguides in chalcogenide glasses are higher than those of etched devices [19], and comparatively small index contrasts might lead to additional bending losses.

Ring resonator structures in PLCs of various electro-optic materials are widely employed as the basis for narrowband filters [29], recirculating delay lines [30], electro-optic modulators [31], and laser cavities [32]. The high sensitivity of the ring cavity to the refractive index of its surroundings is used in biochemical sensors [33]. Cavity enhancement of the pronounced nonlinearities of chalcogenides holds much promise in all-optical signal processing. Ring resonators were fabricated in chalcogenides using a lift-off process, with a reported Q of 10,000 [20]. Recently, loaded (unloaded) Q values of 150,000 (390,000) were achieved in As–Se family glass resonators of 100 μm radius using a nano-imprint fabrication method [21], and unloaded Q of 460,000 was obtained in micro-disc resonators [22]. As_2S_3 racetrack resonators were also fabricated on top of underlying $LiNbO_3$ waveguides [34]. The fabrication of high-Q ring resonators in chalcogenides using direct laser-beam lithography has not yet been reported.

Herein we present the fabrication and characterization of ring resonators in thin As_2S_3 films. Waveguide cores are defined using femtosecond Ti:sapphire laser illumination [10,26]. A large index modification of 0.4 RIU is achieved. The radius of the ring resonators is approximately 1.9 mm, providing a free spectral range (FSR) of 9.1 GHz. The transfer function of the ring resonators corresponds to a loaded (unloaded) Q value of 110,000 (180,000). The results demonstrate the applicability of direct laser-beam lithography to the fabrication of chalcogenide glass PLCs for all-optical signal processing and sensing applications.

2. CHARACTERIZATION OF PHOTO-INDUCED INDEX CHANGES

The layer structure of samples used in this work is shown schematically in Fig. 1. A core As_2S_3 layer of thickness $d_{Ch} = 1.2$ μm was deposited on a silica-on-silicon substrate, by thermal evaporation of a bulk target from a quartz crucible

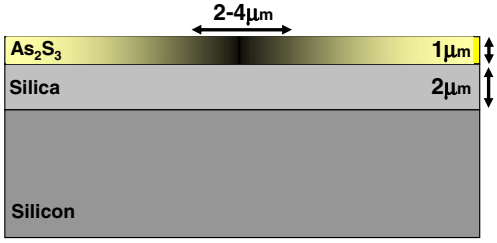

Fig. 1. Schematic illustration of the layer structure of samples used in this work and an illustration of the transverse profile of photo-induced refractive index changes in the core As_2S_3 glass layer.

in a 2×10^{-6} Torr vacuum [35,36]. The thicknesses of the underlying silica layer and of the silicon substrate were $d_{Ox}=2.5$ μm and $d_{Si}=400$ μm, respectively. The refractive indices of As_2S_3, silica, and silicon at 1550 nm wavelength are $n_{Ch}=2.4$ RIU, $n_{Ox}=1.45$ RIU, and $n_{Si}=3.45$ RIU respectively.

Waveguide cores were directly written in the chalcogenide film by femtosecond Ti:sapphire laser illumination, operating at a central wavelength of 810 nm. The sub-bandgap irradiation introduces a permanent increase in the local refractive index through a two-photon, photo-darkening process [10,26]. The writing laser pulses were 200 fs long, and their repetition rate was 80 MHz. The laser beam was focused through a microscope objective lens (numerical aperture of 0.7). The average power of the focused beam was attenuated to 5 mW, and its intensity was 100 kW/cm^2. During illumination, the As_2S_3-coated sample was translated through the focal point of the beam by a computer-controlled, three-axis piezoelectric stage, at 4 μm/s speed.

The definition of ring resonators with ~2 mm radius required the controlled translation of the sample with submicrometer accuracy over several hours. To that end, a closed-loop positioning system was constructed. A fixed camera tracked the exact location of the illumination spot of an external light-emitting diode on the surface of the three-axis stage, and corrected the positioning of the stage motors for possible drifting. In addition, the translation stages were designed for thermal compensation.

The local increase Δn in the refractive index of illuminated regions was estimated using auxiliary transmission measurements, illustrated in Fig. 2. An As_2S_3-coated silica-on-silicon sample was held perpendicular between two collimated fibers. The refractive index within a 0.5 mm × 1 mm pattern in the chalcogenide layer of the sample under test was modified through the direct writing of 150 adjacent linescans, using the above illumination parameters. Light from the output port of an optical vector network analyzer (OVA) at 1550 nm wavelength range was launched towards the bottom surface of the silicon substrate through one fiber, at normal incidence. Light transmitted through the top surface of the sample was collected by the second fiber, and analyzed by the OVA. The

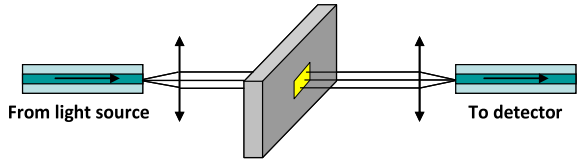

Fig. 2. Schematic illustration of the setup used in measurements of the photo-induced refractive index change in As_2S_3 films.

measurement configuration represents a modification of the Swanepoel method for the determination of the refractive index of thin films [37].

Figure 3 (top) shows the measured transmission through the sample under test as a function of wavelength, both within and outside the irradiated pattern. The transmission through the sample is dominated by reflections at the top and bottom surfaces, which introduce a response of a low-finesse Fabry–Perot etalon. The FSR of the transmission spectrum in reference regions that were not illuminated can be approximated as $FSR_0=\lambda_0^2/(2L_o)$, where λ_0 is the central wavelength and $L_o\equiv d_{Ch}n_{Ch}+d_{Ox}n_{Ox}+d_{Si}n_{Si}$ denotes the optical path length through the sample. The measured FSR_0 is 0.86 nm. The FSR of transmission through the photo-darkened region is modified by

$$\Delta(\mathrm{FSR})\approx(2\mathrm{FSR}_0^2/\lambda_0^2)d_{Ch}\Delta n. \quad (1)$$

Let us denote the wavelengths of maximum transmission as $\{\lambda_m\}$, where m is an integer. Figure 3 (bottom) shows the offsets $\Delta\{\lambda_m\}$ between the transmission spectra of reference and illuminated regions, for 50 FSR periods in the range of 1530–1570 nm. The slope of the $\Delta\{\lambda_m\}$ curve represents Δ(FSR) of 0.338 pm. Direct writing therefore increases the refractive index of the As_2S_3 layer by $\Delta n=0.4$ RIU, to approximately 2.8 RIU. The observed photo-induced Δn is five times larger than that observed in [10]. Note, however, that the accumulated laser irradiation in [J/cm^2] used in this work is orders of magnitude larger. Photo-darkening-induced index changes

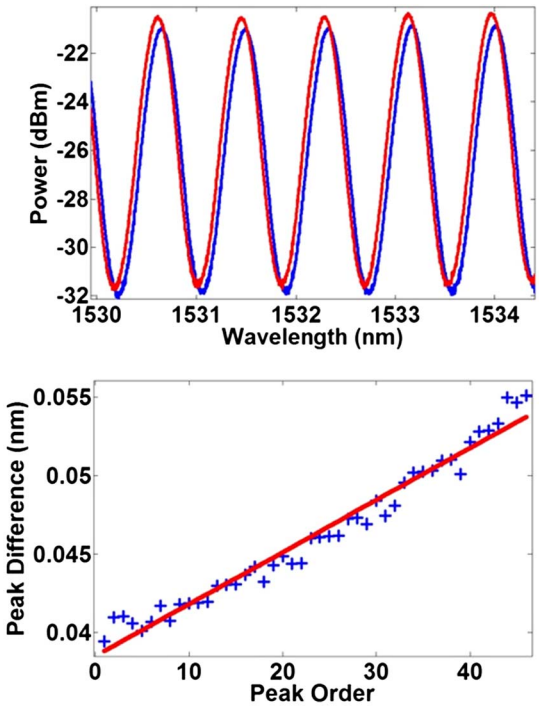

Fig. 3. Top: OVA measurements of the transmission of light through the layers of a silica-on-silicon sample coated with an As_2S_3 film (see Fig. 2). The red (blue) curve corresponds to a region outside (within) a photo-darkened area. Bottom: spectral offset in nanometers between peaks of maximum transmission outside and within the photo-darkened area. The linearly increasing offset corresponds to an increase in the refractive index within the photo-darkened region by 0.4 RIU.

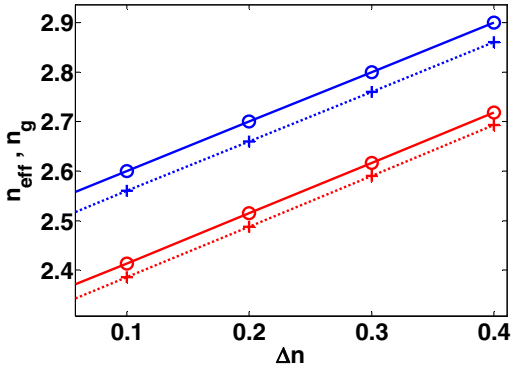

Fig. 4. Calculated effective indices (red) and group indices (blue) of the fundamental modes of directly written waveguides in As_2S_3 thin films, as a function of the photo-induced refractive index change in the core region . Solid (dashed) lines correspond to the TM (TE) mode.

of comparable magnitude in chalcogenides are known in the literature [36,38,39]. Bending losses in rings of millimeter-scale radii and such large Δn values are negligible.

The modal profiles of directly written waveguides at different wavelengths were calculated using COMSOL multiphysics simulations. The waveguide supports multiple transverse-electric (TE) and transverse-magnetic (TM) modes; however, the coupling of light from tapered fibers to higher-order modes is considerably weaker [26] than coupling into the fundamental modes. Figure 4 shows the calculated effective indices n_{eff} and group indices n_g of the fundamental TE and TM modes of a 4-μm-wide waveguide at 1550 nm wavelength, as a function of the photo-induced core Δn. The expected values of the group indices of the fundamental TM and TE modes, with Δn set to 0.4 RIU, are 2.9 and 2.85 RIU, respectively. For the relatively broad core widths of 2–4 μm, and for the comparatively large Δn, the exact profile of graded-index variations has a negligible effect on the calculated indices.

A top-view microscope image of segments of ring and bus waveguides is shown in Fig. 5. The width of the straight bus waveguide core is on the order of 2 μm, whereas that of the ring is approximately 4 μm. The broader width of the ring waveguide is due to its lower scanning speed using alternating x and y translation steps. The separation between the centers of bus and ring waveguides is approximately 2 μm, optimized for maximum extinction ratio (ER) in the transmission frequency response of the devices (see below). Figure 6 shows a top-view image of a ring resonator device of 200 μm radius, with red light coupled in for illustration purposes only. The radius of the specific ring used in subsequent characterization was measured as 1.888 mm, by precise translation of the sample under a microscope with large magnification.

Fig. 5. Top-view microscope image of parts of bus and ring waveguides, directly written in a thin layer of As_2S_3.

Fig. 6. Top view of a ring resonator waveguide, directly written in an As_2S_3 thin film. Red light is coupled from a tapered fiber for illustration purposes only.

3. TRANSFER FUNCTION MEASUREMENTS

The spectral transfer function of the ring resonator was measured using the OVA, with a spectral resolution of 2 pm. Light was coupled in and out of the devices using tapered fibers with a modal radius of 2 μm. The coupling losses to/from the devices at 1550 nm varied between 3 and 5 dB per facet, depending on the facet's quality. Figure 7 shows the OVA measurement of the infinite impulse response of the ring resonator in the time domain. The 110 ps delay between successive impulses corresponds to a group index of 2.8 RIU, in general agreement with simulations. The measured group delay corresponds to a photo-induced Δn value of 0.3–0.35 RIU (see Fig. 4). The attenuation between successive impulses is given by $|\kappa|^2 \cdot \exp(-\alpha L)$, where κ is the coupling coefficient between the bus and ring waveguides, α denotes the loss coefficient per unit length, and L is the circumference of the ring. The measurements suggest that $|\kappa|^2 \cdot \exp(-\alpha L) = 7.2$ dB.

Figure 8 (top) shows the measured spectral power transfer function of the ring resonator. A FSR of 9.1 GHz is observed, with an ER that reaches 25 (14 dB). Figure 8 (bottom) shows a magnified view of one spectral transmission notch. The full width at half maximum (FWHM) of the transmission notches is 14 pm, which corresponds to a loaded Q value of approximately 110,000. The unloaded Q value and the loss coefficient α may be estimated using the following relations [40]:

$$Q_{\text{int}} = 2Q_{\text{loaded}}/\left(1 + \sqrt{\text{ER}^{-1}}\right) = 180,000, \tag{2}$$

$$\alpha = (2\pi n_g)/(Q_{\text{int}}\lambda_0) = 2.7 \text{ dB/cm}, \tag{3}$$

where Q_{loaded} and Q_{int} denote the loaded and unloaded Q values, respectively. The relatively high value of Q is an order of

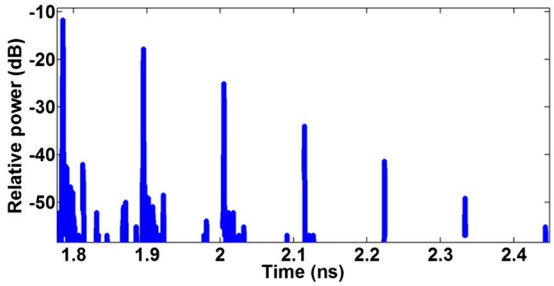

Fig. 7. OVA measurement of the temporal impulse response of a ring resonator of 1.888 mm radius, directly written in a thin film of As_2S_3.

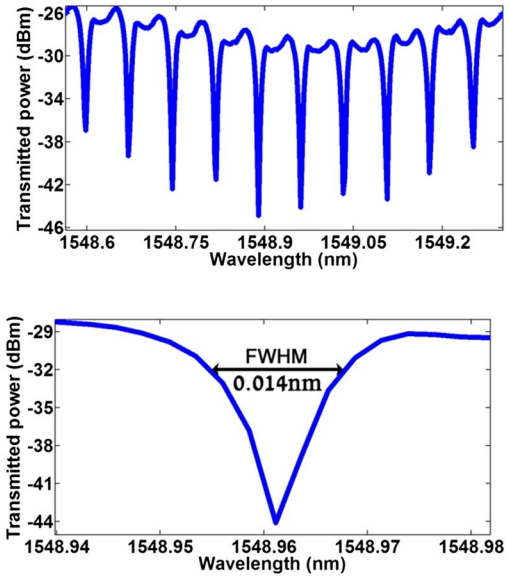

Fig. 8. Top: OVA measurement of the spectral power transfer function of a ring resonator of 1.888 mm radius, directly written in a thin film of As_2S_3. Bottom: magnified view of a single transmission notch, with a FWHM of 0.014 nm.

magnitude better than that reported using a lift-off fabrication process [20], and a factor of 2 lower than the values obtained recently in As–Se glasses using thermal nanoimprinting [21,22].

Figure 9 shows the spectral power transfer functions of the ring resonator at different temperatures T of an actively controlled mount. The observed thermal offset of a given resonance wavelength λ_r was $d\lambda_r/dT = 0.022$ nm/°C. The thermal offset is given by

$$d\lambda_r/dT = (\alpha_T + n_T/n_g)\lambda_r, \tag{4}$$

where $n_T \equiv dn_{Ch}/dT$ is the thermo-optic coefficient of As_2S_3 and $\alpha_T \equiv (dL/dT)/L$ denotes the coefficient of linear thermal expansion. Values of $n_T = 50 \times 10^{-6}$ RIU/°C [41] and $\alpha_T = 21$ ppm/°C [42] appear in the literature. Based on these values, a larger thermal change of 0.060 nm/°C in the resonance wavelength could be expected. The reasons for this difference require further investigation. A possible explanation could be

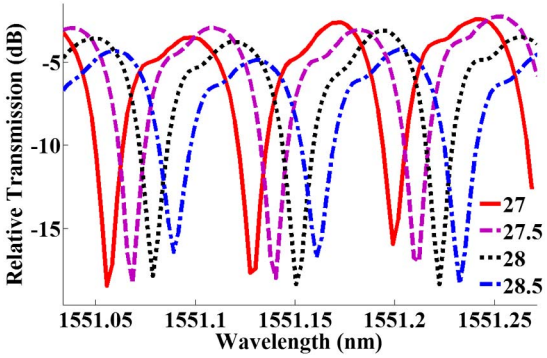

Fig. 9. OVA measurements of the spectral power transfer function of a ring resonator of 1.888 mm radius, at several temperatures (in °C, see legend). The resonance wavelengths are offset by 0.022 nm/°C.

due to thermal expansion of the entire layer structure, which might be different from that of bulk As_2S_3.

The transfer function of the device was monitored over more than one year of storage in a standard laboratory environment. No changes were noted in Q_{loaded} or ER. The devices support a coupled average power of 200 mW, and 500-ns-long pulses with coupled peak power of 2 W, without damage.

4. CONCLUSION

In summary, this work provides the first report, to the best of our knowledge, of high-Q ring resonators in As_2S_3 glass PLCs, fabricated using direct laser-beam writing. The simple fabrication of high-quality resonators in highly nonlinear media carries much promise for all-optical signal processing applications. Ongoing work is being dedicated to the fabrication of resonators having different values of Δn, and to attempts to reduce losses. Losses may be improved with the deposition of upper capping layers, such as silica, which might prevent oxidization of the chalcogenide glass surface. Lastly, nonlinear propagation effects in the resonator devices are being investigated.

ACKNOWLEDGMENTS

This work is dedicated to the memory of Prof. Victor Lyubin (1928–2013), of Ben-Gurion University of the Negev, Beer-Sheva, Israel, a pioneer and leader in research of chalcogenide glasses. Prof. Lyubin was responsible for the deposition of As_2S_3 films used in this research. S. Levy and A. Zadok acknowledge the support of the Israeli Science Foundation (ISF), under grant 635/10.

REFERENCES

1. B. T. Kolomiets, "Vitreous semiconductors I," Phys. Status Solidi **7**, 359–372 (1964).
2. B. T. Kolomiets, "Vitreous semiconductors II," Phys. Status Solidi **7**, 713–731 (1964).
3. R. Frerichs, "New optical glasses with good transmission in the infrared," J. Opt. Soc. Am. **43**, 1153–1157 (1953).
4. K. Ogusu, J. Yamasaki, S. Maeda, M. Kitao, and M. Minakata, "Linear and nonlinear optical properties of Ag-As-Se chalcogenide glasses for all-optical switching," Opt. Lett. **29**, 265–267 (2004).
5. J. S. Sanghera, I. D. Aggarwal, L. B. Shaw, C. M. Florea, P. Pureza, V. Q. Nguyen, F. Kung, and I. D. Aggarwal, "Nonlinear properties of chalcogenide glass fibers," J. Optoelectron. Adv. Mater. **8**, 2148–2155 (2006).
6. A. Zakery and S. R. Elliot, "Optical properties and applications of chalcogenide glasses: a review," J. Non-Cryst. Solids **330**, 1–12 (2003).
7. E. Owen, A. P. Firth, and P. J. S. Ewen, "Photo-induced structural and physico-chemical changes in amorphous chalcogenide semiconductors," Philos. Mag. B **52**, 347–362 (2006).
8. J. D. Musgraves, K. Richardson, and H. Jain, "Laser-induced structural modification, its mechanisms, and applications in glassy optical materials," Opt. Mater. Express **1**, 921–935 (2011).
9. V. I. Mikla, "Photoinduced structural changes and related phenomena in amorphous arsenic chalcogenides," J. Phys. Condens. Matter **8**, 429–448 (1996).
10. A. Zoubir, M. Richardson, C. Rivero, A. Schulte, C. Lopez, and K. Richardson, "Direct femtosecond laser writing of waveguides in As_2S_3 thin films," Opt. Lett. **29**, 748–750 (2004).
11. Y. Kaganovskii, D. L. Beke, S. Charnovych, S. Kokenyesi, and M. L. Trunov, "Inversion of the direction of photo-induced mass transport in As20Se80 films: experiment and theory," J. Appl. Phys. **110**, 063502 (2011).

12. A. Saliminia, T. V. Galstian, and A. Villeneuve, "Optical field-induced mass transport in As_2S_3 chalcogenide glasses," Phys. Rev. Lett. **85**, 4112–4115 (2000).
13. M. L. Trunov, P. M. Lytvyn, P. M. Nagy, and O. M. Dyachyns'ka, "Real-time atomic force microscopy imaging of photoinduced surface deformation in AsSe chalcogenide films," Appl. Phys. Lett. **96**, 111908 (2010).
14. M. L. Trunov, P. M. Lytvyn, and O. M. Dyachyns'ka, "Alternating matter motion in photoinduced mass transport driven and enhanced by light polarization in amorphous chalcogenide films," Appl. Phys. Lett. **97**, 031905 (2010).
15. B. J. Eggleton, B. Luther-Davies, and K. Richardson, "Chalcogenide photonics," Nat. Photonics **5**, 141–148 (2011).
16. V. Ta'eed, N. J. Baker, L. Fu, K. Finsterbusch, M. R. E. Lamont, D. J. Moss, H. C. Nguyen, B. J. Eggleton, D.-Y. Choi, S. Madden, and B. Luther-Davies, "Ultrafast all-optical chalcogenide glass photonic circuits," Opt. Express **15**, 9205–9221 (2007).
17. M. D. Pelusi, F. Luan, S. Madden, D.-Y. Choi, D. A. Bulla, B. Luther-Davies, and B. J. Eggleton, "Wavelength conversion of high-speed phase and intensity modulated signals using a highly nonlinear chalcogenide glass chip," IEEE Photon. Technol. Lett. **22**, 3–5 (2010).
18. M. Galili, J. Xu, H. C. H. Mulvad, L. K. Oxenløwe, A. T. Clausen, P. Jeppesen, B. L. Davies, S. Madden, A. Rode, D. Y. Choi, M. Pelusi, F. Luan, and B. J. Eggleton, "Breakthrough switching speed with an all-optical chalcogenide glass chip: 640 Gbit/s demultiplexing," Opt. Express **17**, 2182–2187 (2009).
19. S. J. Madden, D.-Y. Choi, D. A. Bulla, A. V. Rode, B. Luther-Davies, V. G. Ta'eed, M. D. Pelusi, and B. J. Eggleton, "Long, low loss etched As_2S_3 chalcogenide waveguides for all-optical signal regeneration," Opt. Express **15**, 14414–14421 (2007).
20. J. Hu, N. Carlie, L. Petit, A. Agarwal, K. Richardson, and L. Kimerling, "Demonstration of chalcogenide glass racetrack microresonator," Opt. Lett. **33**, 761–763 (2008).
21. Y. Zou, D. Zhang, H. Lin, L. Li, L. Moreel, J. Zhou, Q. Du, O. Ogbuu, S. Danto, J. D. Musgraves, K. Richardson, K. D. Dobson, R. Birkmire, and J. Hu, "High-performance, high-index-contrast chalcogenide glass photonics on silicon and unconventional non-planar substrate," Adv. Opt. Mater. **2**, 478–486 (2014).
22. L. Li, H. Lin, S. Qiao, Y. Zou, S. Danto, K. Richardson, J. D. Musgraves, N. Lu, and J. Hu, "Integrated flexible chalcogenide glass photonic devices," Nat. Photonics **8**, 643–649 (2014).
23. K. Turcotte, J. M. Laniel, A. Villeneuve, C. Lopez, and K. Richardson, "Fabrication and characterization of chalcogenide optical waveguides," in *Integrated Photonics Research*, T. Li, ed., Vol. **45** of OSA Trends in Optics and Photonics (Optical Society of America, 2000), paper IFH4.
24. O. M. Efimov, L. B. Glebov, K. A. Richardson, E. Van Stryland, T. Cardinal, S. H. Park, M. Couzi, and J. L. Bruneel, "Waveguide writing in chalcogenide glasses by a train of femtosecond laser pulses," Opt. Mater. (Amsterdam) **17**, 379–386 (2001).
25. X. Gai, T. Han, A. Prasad, S. Madden, D.-Y. Choi, R. Wang, D. Bulla, and B. Luther-Davies, "Progress in optical waveguides fabricated from chalcogenide glasses," Opt. Express **18**, 26635–26646 (2010).
26. S. Levy, V. Lyubin, M. Klebanov, J. Scheuer, and A. Zadok, "Stimulated Brillouin scattering amplification in centimeter-long directly written chalcogenide waveguides," Opt. Lett. **37**, 5112–5114 (2012).
27. A. Saliminia, A. Villeneuve, T. V. Galstyan, S. LaRochelle, and K. Richardson, "First-and second-order Bragg gratings in single-mode planar waveguides of chalcogenide glasses," J. Lightwave Technol. **17**, 837–842 (1999).
28. N. Hô, M. C. Phillips, H. Qiao, P. J. Allen, K. Krishnaswami, B. J. Riley, T. L. Myers, and N. C. Anheier, Jr., "Single-mode low-loss chalcogenide glass waveguides for the mid-infrared," Opt. Lett. **31**, 1860–1862 (2006).
29. Q. Li, M. Soltani, S. Yegnanarayanan, and A. Adibi, "Design and demonstration of compact, wide bandwidth coupled-resonator filters on a siliconon- insulator platform," Opt. Express **17**, 2247–2254 (2009).
30. H. Park, J. P. Mack, D. J. Bluementhal, and J. E. Bowers, "An integrated recirculating optical buffer," Opt. Express **16**, 11124–11131 (2008).
31. Q. Xu, B. Schmidt, S. Pradhan, and M. Lipson, "Micrometre scale silicon electro-optic modulator," Nature **435**, 325–327 (2005).
32. W. Fang, R. Jones, H. Park, O. Cohen, O. Raday, M. J. Paniccia, and J. E. Bowers, "Integrated AlGaInAs-silicon evanescent racetrack laser and photodetector," Opt. Express **15**, 2315–2322 (2007).
33. M. Armani, R. P. Kulkarni, S. E. Fraser, R. C. Flagan, and K. J. Vahala, "Label-free single-molecule detection with optical microcavities," Science **317**, 783–787 (2007).
34. M. E. Solmaz, D. B. Adams, W. C. Tan, W. T. Snider, and C. K. Madsen, "Vertically integrated As_2S_3 ring resonator on LiNbO3," Opt. Lett. **34**, 1735–1737 (2009).
35. I. Abdullhalim, M. Gelbaor, M. Klebanov, and V. Lyubin, "Photo-induced phenomena in nano-dimentional glassy As_2S_3 films," Opt. Mater. Express **1**, 1192–1201 (2011).
36. B. Spektor, J. Shamir, V. Lyubin, and M. Klebanov, "Recording on As_2S_3 glassy films by pulsed and continuous illumination—optical evaluation and comparison," Opt. Eng. **42**, 3279–3284 (2003).
37. R. Swanepoel, "Determination of the thickness and optical constants of amorphous silicon," J. Phys. E **16**, 1214–1222 (1983).
38. G. Pfeiffer, M. A. Paesler, and S. C. Agrawal, "Reversible photodarkening of amorphous arsenic chalcogens," J. Non-Cryst. Solids **130**, 111–143 (1991).
39. M. A. Iovu, M. S. Iovu, D. V. Harea, E. P. Colomeico, and V. G. Ciorba, "Light induced phenomena in amorphous $As_{100-x}Sex$ and $As_{40}Se_{60}$:Sn thin films," Proc. SPIE **6635**, 663509 (2007).
40. L. W. Luo, G. S. Wiederhecker, J. Cardenas, C. Poitras, and M. Lipson, "High quality factor etchless silicon photonic ring resonators," Opt. Express **19**, 6284–6289 (2011).
41. A. Saliminia, T. Galstian, A. Villeneuve, K. Le Foulgoc, and K. Richardson, "Temperature dependence of Bragg reflectors in chalcogenide As_2S_3 glass slab waveguides," J. Opt. Soc. Am. B **17**, 1343–1348 (2000).
42. G. Tao, "Multimaterial fibers in photonics and nanotechnology," Ph.D. dissertation (University of Central Florida, 2014).